Bioorganic Chemistry 93 (2019) 103315

Contents lists available at ScienceDirect

Bioorganic Chemistry

journal homepage: www.elsevier.com/locate/bioorg

Adapalene inhibits ovarian cancer ES-2 cells growth by targeting glutamic-oxaloacetic transaminase 1

Qiqi Wang[b,1], Qingzhe Zhang[a,1], Shanshan Luan[a,1], Kaiyin Yang[a], Mengzhu Zheng[a,*], Kezhen Li[c,*], Lixia Chen[b,*], Hua Li[a,*]

[a] Hubei Key Laboratory of Natural Medicinal Chemistry and Resource Evaluation, School of Pharmacy, Tongji Medical College, Huazhong University of Science and Technology, Wuhan 430030, China

[b] Wuya College of Innovation, Key Laboratory of Structure-Based Drug Design & Discovery, Ministry of Education, Shenyang Pharmaceutical University, Shenyang 110016, China

[c] Cancer Biology Center, Tongji Hospital, Tongji Medical College, Huazhong University of Science and Technology, Wuhan 430030, China

ARTICLE INFO

Keywords:
Adapalene
GOT1 inhibitor
Ovarian cancer
Drug repurposing

ABSTRACT

Glutamic-oxaloacetic transaminase 1 (GOT1) regulates cellular metabolism through coordinating the utilization of carbohydrates and amino acids to meet nutrient requirements for sustained proliferation. As such, the GOT1 inhibitor may provide a new strategy for the treatment of various cancers. Adapalene has been approved by FDA for the treatment of acne, pimples and pustules, and it may also contribute to the adjunctive therapy for advanced stages of liver and colorectal cancers. In this work, we first examined the enzyme inhibition of over 500 compounds against GOT1 *in vitro*. As a result, Adapalene effectively inhibited GOT1 enzyme in a non-competitive manner. MST and DARTS assay further confirmed the high affinity between Adapalene and GOT1. Furthermore, the growth and migration of ovarian cancer ES-2 cells were obviously inhibited by the treatment of Adapalene. And it induced the apoptosis of ES-2 cells according to Western blot and Hoechst 33258 straining. In addition, molecular docking demonstrated that Adapalene coordinated in an allosteric site of GOT1 with low binding energy. Furthermore, knockdown of GOT1 in ES-2 cells decreased their anti-proliferative sensitivity to Adapalene. Together, our data strongly suggest Adapalene, as a GOT1 inhibitor, could be regarded as a potential drug candidate for ovarian cancer therapy.

1. Introduction

Ovarian cancer is one of the three leading gynecological malignancies and the fifth principal cause of females' cancers [1]. Insidious growth, highly frequent metastasis and rapid development of drug resistance are important features of ovarian cancer which lead to its low 5-year survival rates [2]. It was reported that 62.4% of new ovarian cancer cases finally died in the United States during 2016 [3]. Therefore, more effective therapeutics is urgently needed to cure ovarian cancer.

Most cancers depend highly on the levels of aerobic glycolysis, known as Warburg effect, for their sustained growth and proliferation [4,5]. However, transformation of metabolism methods to meet the biosynthetic requirements of cells is a hallmark of tumor cells [6]. Various cancer cells such as pancreatic cancer cells and breast adenocarcinomas exhibited addiction to glutamine (Gln) which is delaminated to glutamate and further converted into alpha-ketoglutarate (α-KG), fueling the TCA cycle as a carbon source for the biosynthesis of nucleotides, non-essential amino acids, and hexosamines [7]. However, the subsequent studies showed that some cancer cells metabolized Gln in a different manner from canonical model that Gln-derived aspartate (Asp) was transported into the cytoplasm, in which glutamic-oxaloacetic transaminase 1 (GOT1) catalyzed the conversion of aspartate (Asp) and α-KG into oxaloacetate (OAA) and glutamate (Glu). Since the selective inhibition of GOT1 decreases the proliferation of cancer cells, GOT1 represents a valid molecular target for the development of antitumor agents [8].

However, the inhibitors of GOT1 are relatively scarce, and the

Abbreviations: GOT1, glutamic-oxaloacetic transaminase 1; MST, microscale thermophoresis; IPTG, isopropyl β-D-1-thiogalactopyranoside; ADA, adapalene; PVDF, polyvinylidene fluoride

* Corresponding authors.
E-mail addresses: mengzhu_zheng@hust.edu.cn (M. Zheng), tjkeke@126.com (K. Li), syzyclx@163.com (L. Chen), li_hua@hust.edu.cn (H. Li).

[1] These authors contributed equally to this work.

https://doi.org/10.1016/j.bioorg.2019.103315
Received 21 April 2019; Received in revised form 13 August 2019; Accepted 25 September 2019
Available online 26 September 2019

researches were restricted to the inhibitions of enzyme activity and cell proliferation, and no any GOT1 inhibitor has enter clinical research yet. Our group is dedicated to the discovery of novel potent and selective GOT1 inhibitors. Herein, we first found that an approved drug Adapalene (ADA, 6-[3-(1-adamantyl)-4-methoxyphenyl]-2-naphtoic acid) could selectively inhibit the activity of GOT1, and further suppress the proliferation of ovarian cancer ES-2 cells. Adapalene as the third generation of retinoids, is clinically used in the topic therapy of acne vulgaris. Although pharmacological properties of ADA have been extensively studied [9–12], and it showed inhibitions on the proliferation of Hela, HepG2 and CC-531 cells [13–15], its antitumor mechanism is still unclear. In the field of anti-cancer research, adapalene induces apoptosis by altering the ratio of bax/bcl-2 in liver cancer cells, and induces cell cycle arrest in G1 phase of colorectal cancer [13–15]. But the real target of ADA anti-cancer remains to be explored. In this work, we identified that ADA suppressed the proliferation of ES-2 cells by specific inhibiting GOT1, which provides a novel strategy for ovarian cancer treatment.

2. Experimental section

2.1. Reagent

Adapalene (106685-40-9) was purchased from meilunbio (China), dissolved in dimethyl sulfoxide (DMSO) and deposited at −20 °C refrigerator. Antibodies of GOT1, β-actin, Bcl-2 and PARP were purchased commercially from ABclonal (China), and goat anti-rabbit IgG was obtained from ABclonal (China).

2.2. Cell culture

Cells were obtained from American Type Culture Collection (ATCC) and cultured in a humidified incubator at 37 °C within a 5% CO2 atmosphere. The culture medium was DMEM containing 10% (v/v) fetal bovine serum (FBS), 1% (v/v) 100 Xpenicillin/streptomycin solution [16].

2.3. Cell viability assays

MTT assay was performed for measuring of cells viability. Briefly, 6000 cells/well were plated in 96-well plates, and then treated with 0.1% DMSO as a solvent control or various concentration gradients (0–200 μM) of ADA. After 24 h treatment, the supernatant was discarded carefully and 100 μL/wells MTT solution (5 mg/mL) was added. Subsequently, the plates were incubated at 37 °C for another 4 h, followed by addition of DMSO (100 μL/well) to dissolve the formed formazan crystals. The results were assessed with a microplate reader at 490 nm [17].

2.4. Expression and purification of GOT1

Firstly, the gene of homo GOT1 (Gene ID: 2805) obtained from TSINGKE (Wuhan. China), was cloned into the pET28a vector (Novagen) containing a 6 His-tag coding region. After validated by sequencing, the recombinant plasmids were transformed into *Escherichia coli* strain BL21 (DE3) and cultured in LB medium at 37 °C. The cells were induced with isopropyl-D-thiogalactopyranoside (IPTG) (0.4 mM) at 20 °C for 20 hand then harvested by centrifugation. The lysis buffer (100 mM Tris-HCL, pH 8.8, 200 mM NaCl, 1% TritonX-100, 10% Glycerol) was then used to re-suspend the cells on ice. The Ultrasonic Cell Disruptor was applied to disrupt cells. 21500 rpm centrifuge for 40 min to remove cellular debris. The GOT1 protein was purified by Ni-agarose affinity resin with washing buffer (20 mM Tris-HCL, pH 8.8, 200 mM NaCl, 10 mM imidazole) and elution buffer (20 mM Tris-HCL, pH 8.8, 200 mM NaCl, 150 mM imidazole). Finally, the protein was further purified by gel filtration in buffer containing 200 mM NaCl and 100 mM Tris-HCL pH 8.8 [18].

2.5. GOT1 inhibitory activity assay

The effectiveness of compounds on GOT1 was assessed using purified homo recombinant GOT1. Total 100 μL reaction mixture, containing 4 mM aspartic acid, 1 mM α-KG, 1 units/mL malate dehydrogenase, 1 mM NADH and 0.1 mg/mL homo recombinant GOT1, was assessed at 340 nm by a microplate reader. Results were analyzed using GraphPad prism7 (GraphPad software, Inc. CA, USA) based on the maximum linear change of NADH absorbance.

2.6. Microscale thermophoresis (MST) assay

Homo GOT1 protein was diluted with 20 mM HEPES (pH 7.5) to 10 μM and labelled with the Monolith NTTM Protein Labeling Kit RED (Cat # L001). 1 mM Adapalene was used as the initial concentration for subsequent gradient dilution. Mixed the different concertation of ADA with GOT1 and incubated for30 min at room temperature. The specimens were loaded and measured on a Monolith NT.115 instrument (Nano Temper Technologies, München, Germany). The dissociation constant (K_d) values were fitted by the NT Analysis software (Nano Temper Technologies, München, Germany) [19].

2.7. Drug affinity responsive target stability (DARTS) assay

For the DARTS assay, 1 mg/mL GOT1 protein was treated with different concentration of Adapalene and incubated with 1 μg/mL pronase at 37 °C for 30 min. The extent of hydrolyzation of each specimen was measured by Western blot. The Image J was used for quantitative analysis [20].

2.8. Molecular docking

The resolved crystal structure of homo GOT1 (PDB ID: 3II0) was obtained from the Protein Data Bank (http://www.rcsb.org/). The docking was carried out through ICM 3.8.2 modeling software implemented in Intel i7 4960 processor (MolSoft LLC, San Diego, CA). The key residues located in ligand binding pocket were selected via graphical tools within ICM software, creating the grid box of the ligand docking. Prior to the docking calculation, the potential energy map of the receptor was computed with default parameters. Subsequently, ligands were imported into ICM software and the index file was created simultaneously. Based on the Monte Carlo procedure 30, the various conformations were sampled. Finally, the ligands of the most favorable pose with the lowest-energy were selected [21].

2.9. Colony formation assay

200 ES-2 cells/well were plated in 6-well plates for 24 h, and then treated with ADA. The plates were cultured in cell culture incubators for 10–14 days and replaced medium with new ADA-containing DMEM every three days. When forming the visible cloning, clones were fixed with 4% paraformaldehyde for 15 min and stained with 1% crystal violet for 15 min. After washing with PBS for three times, stained clones containing more than 50 cells were counted. The formal that clone number/total cell number × 100% was used to calculate the cloning efficiency [22].

2.10. EdU proliferation assay

The EdU proliferation assay kit was obtained from Ribobio (China). Briefly, approximately 6000 cells/well were plated into 96-well plates for 24 h and were treated to various concentration of ADA for another 24 h, staining with 50 μM EdU for 2 h. After fixed with 4% paraformaldehyde for 30 min, glycine and TritonX-100were added to the

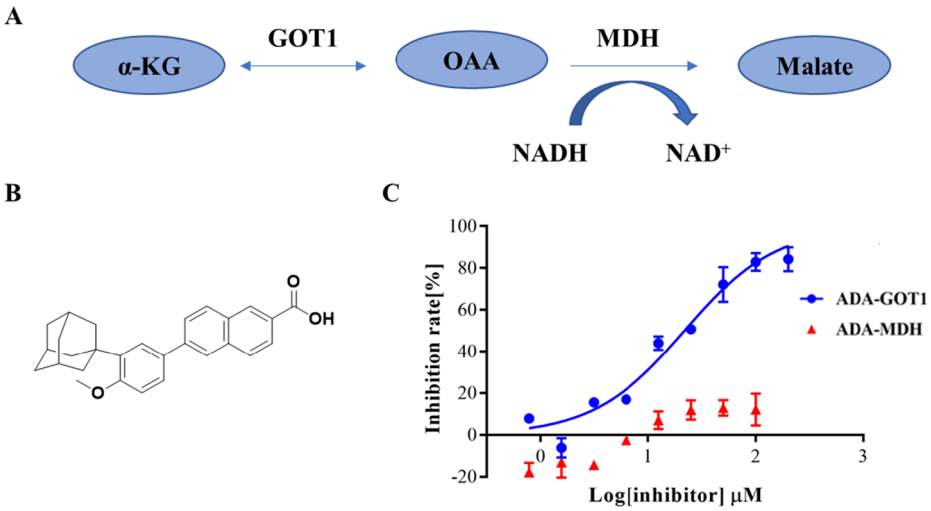

Fig. 1. *In vitro* enzyme inhibition assay. (A) The schematic diagram of enzyme activity reaction. (B) The chemical structural formula of ADA. (C) The selective inhibition of ADA on GOT1 and MDH.

wells respectively according the protocol. Finally, the wells were stained with Hoechst 33342 and imaged using a fluorescence microscopy (Nikon) [16].

2.11. Transwell migration assay

For the transwell migration assay, 8.0 μm Transwell Permeable Supports was obtained from Corning (USA). The upper chamber precoated were added with 100 μL serum-free medium containing 5×10^4 ES-2 cells after 600 μL medium containing 10% FBS and different concentrations ADA (0–40 μM) were added into the lower chamber. Eventually, cells that invaded to the bottom of membrane were fixed by 4% methanol for 15 min after incubation for 16 hand then stained with 0.4% crystal violet solution for 30 min. The cells on the bottom surface of the membrane were captured using a digital microscopy (Nikon, Japan) [23].

2.12. Wound scratch assay

ES-2 cells were planked in 6-well plates with 5×10^5 cells/well for 24 h. When cells density reached to 85%, a sterilized 10 μL micro pipette tip was applied to make three straight scratches per well. The plates were then washed with PBS to remove the floating cells before the ADA (0–40 μM) added. The cell migration extent was imaged by a digital microscopy at 0 and 24 h after the scratches were made [24].

2.13. Hoechst 33258 straining

For the Hoechst 33258 straining, cells were plated in 96 wells with 5×10^3/well for 24 h, ES-2 cells were treated with Adapalene for another 16 h and stained with Hoechst 33258 for 30 min at room temperature in the dark. The changes of apoptotic morphological were measured by a fluorescence microscope (Nikon, Japan) [25].

2.14. Western blot assays

The proteins of GOT1, PARP, Bcl-2 and β-actin were measured by Western blot assay. Cell samples were resuspended in RIPA lysis buffer containing 0.1 mM PMSF, the samples were vortexed for 10 s every ten minutes and vortexed 3 times, and then centrifuged at 13000 rpm for 10 min. The concentration of supernatants was measured by BCA protein assay kit purchased from Beyotime (China). An equal amount of protein was resolved by performing 12% SDS-PAGE and then transferred to a same size of polyvinylidene difluoride (PVDF) membrane. After blocking with 5% (w/v) skimmed milk dissolved by TBST buffer at room temperature for 1 h, the PVDF membrane incubated with specific above protein primary antibodies overnight at 4 °C, followed by incubation with corresponding horseradish peroxidase-conjugated secondary antibody at room temperature for 2 h. Finally, the Western blots were probed by enhanced chemiluminescence (ECL) [26].

2.15. siRNA knockdown of GOT1

Briefly, siRNA was purchased from General Biosystems company. The ES-2 cells were transfected with 50 nM siKGA (siRNA1, siRNA2 and siRNA3) or siCtrl using Hieff TransTM Liposomal Transfection reagent (YEASEN), according to the manufacturer's instructions. Subsequently, the cells were analyzed by a Western blot assay.

GOT1 (human) siRNA-1 Forward: 5′ to 3′ UGA AGA AAG UGG AGC AGA ATT
GOT1 (human) siRNA-1 Reverse: 5′ to 3′ UUC UGC UCC ACU UUC UUC ATT
GOT1 (human) siRNA-2 Forward: 5′ to 3′ UGG AGA AGA UCG UGC GGA UTT
GOT1 (human) siRNA-2 Reverse: 5′ to 3′ AUC CGC ACG AUC UUC UCC ATT
GOT1 (human) siRNA-3 Forward: 5′ to 3′ CCU GAA UGA UCU GGA GAA UTT
GOT1 (human) siRNA-3 Reverse: 5′ to 3′ AUU CUC CAG AUC AUU CAG GTT

3. Results

3.1. The selective inhibition of ADA on GOT1 activity

To find novel GOT1 inhibitors, the preliminary biological evaluation against GOT1 protein *in vitro* was carried out, and over 500 compounds from the approved drug library were screened. The schematic diagram of enzyme activity reaction was given in Fig. 1A. The initial concentration was selected as 50 μM, and compounds with inhibition activity greater than 50% were selected for further verification. As a result, ADA, an approved drug (Fig. 1B), showed an obvious inhibitory effect on GOT1 (IC_{50} = 21.79 ± 1.08 μM). Meanwhile, in Fig. 1C, the change of NADH level was caused by the inhibition of GOT1, but not MDH (IC_{50} > 200 μM). ADA exhibited a specific inhibitory effect on GOT1, which attracted our attention for further study.

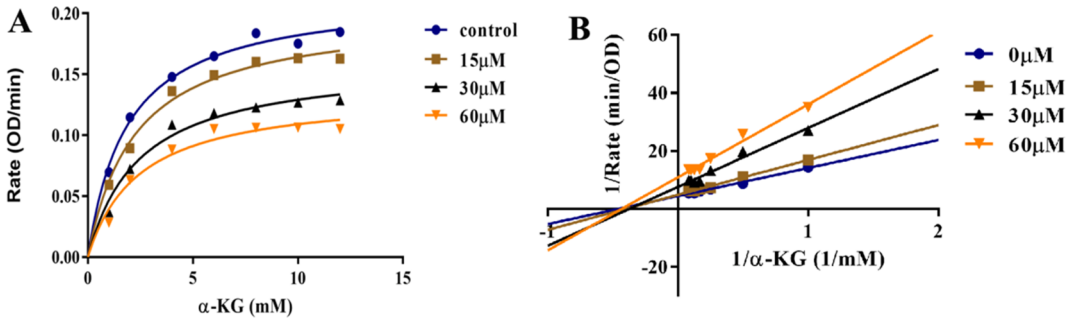

Fig. 2. A steady-state enzyme kinetics study of ADA to GOT1. (A) α-KG saturation profiles for GOT1 at a range of concentrations of ADA. (B) Line weaver–Burk double-reciprocal representation of the α-KG saturation profiles for GOT1at a range of concentrations of ADA.

Table 1
Kinetic parameters of ADA treatment on GOT1.

ADA (μM)	Km (μM)[a]	Vmax (△OD/min)
0	1.89 ± 0.22	0.22 ± 0.01
15	2.12 ± 0.27	0.20 ± 0.03
30	2.45 ± 0.46	0.16 ± 0.03
60	2.44 ± 0.62	0.13 ± 0.01

[a] The Km value represents the concentration of α-KG at half the maximum enzyme reaction rate. The value was automatically calculated by the curve fitting, and presents as means ± SD for three experiments.

3.2. A steady-state enzyme kinetics study of ADA to GOT1

To assess the mode of inhibition caused by ADA, enzyme kinetics has been measured. As a result, V_{max} was decreased by ADA treatment in a dose-dependent way (Fig. 2A). While, ADA displayed little effect on the kinetic constant K_m for α-KG consumption (Table 1 and Fig. 2B). These data indicated that ADA inhibited GOT1 in a non-competitive manner against the substrate α-KG.

3.3. Specific binding of ADA with GOT1 in vitro

Both Microscale thermophoresis (MST) and Drug Affinity Responsive Targeting Stability (DARTS) assays were employed to further validate the interaction between ADA and GOT1. For MST, the fluorescent changes of molecules during thermophoresis were detected to quantify protein-small molecule interactions. In this study, the equilibrium dissociation constant (K_d) value of ADA and GOT1 was measured and elucidated as 195.00 ± 14.10 μM, which indicated a relatively strong binding affinity (Fig. 3A). Furthermore, DARTS is a detection based on the principle that small molecules can prevent target protein from degrading by proteolytic enzymes, as shown in Fig. 3B, ADA significantly mitigated the proteolysis of GOT1 induced by pronase. Those results demonstrated that ADA could directly bind with GOT1.

3.4. Molecular docking elucidated the binding mode of ADA with GOT1

In order to further elucidate the binding mode of ADA with GOT1, molecular docking was carried out by using ICM 3.8.2 modeling software (MolSoft LLC, San Diego, CA) [21]. Ligand binding pocket residues were selected by using graphical. The lowest-energy binding conformation of ADA with the enzyme was shown as Fig. 4. Docking results demonstrated that the compound bind to an allosteric site of the enzyme (Fig. 4A). The binding pocket of ADA was located in the back site of the active site, shaped like a hammer with handle, where several hydrophobic amino acids, including Cys83, Leu87, Leu311, Ser312, Pro314, Phe317, Trp320 and Thr321 form a relatively hydrophobic pocket to contain the adamantane of the compound. The key hydrophobic interaction was formed by Pro314 with the adamantine part, and Phe317 formed an obvious stacking with the benzene ring of the anisole part. Hydrogen bonds were predicted between ADA with Asn233 (Fig. 4B). It seems that two key hydrophobic interactions and the hydrogen binding fix the compound in this allosteric site and direct it in the right orientation. Predicted allosteric binding was consistent with the non-competitive inhibition of ADA against the substrate of GOT1.

3.5. The inhibition of ADA on cancer cells

GOT1 protein levels were measured by western blot in cancer cell lines derived from various cancer types, such as pancreatic cancer (SW1990, Aspc-1), breast cancer (mm-231, mm-468, MCF-7), liver

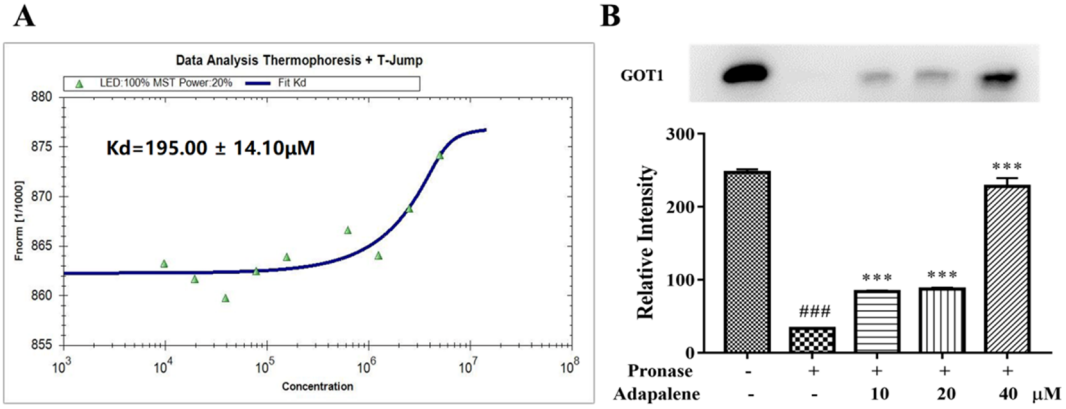

Fig. 3. The combining capacity of ADA with GOT1. (A) Binding affinity of ADA with GOT1 by MST in standard treated capillaries (B) DARTS assay was performed on GOT1-homo protein. ###indicated effectively proteolysis of GOT1 ($p < 0.001$) treated with pronase compared with the one untreated, and *** indicated strongly mitigation of GOT1 proteolysis ($p < 0.001$).

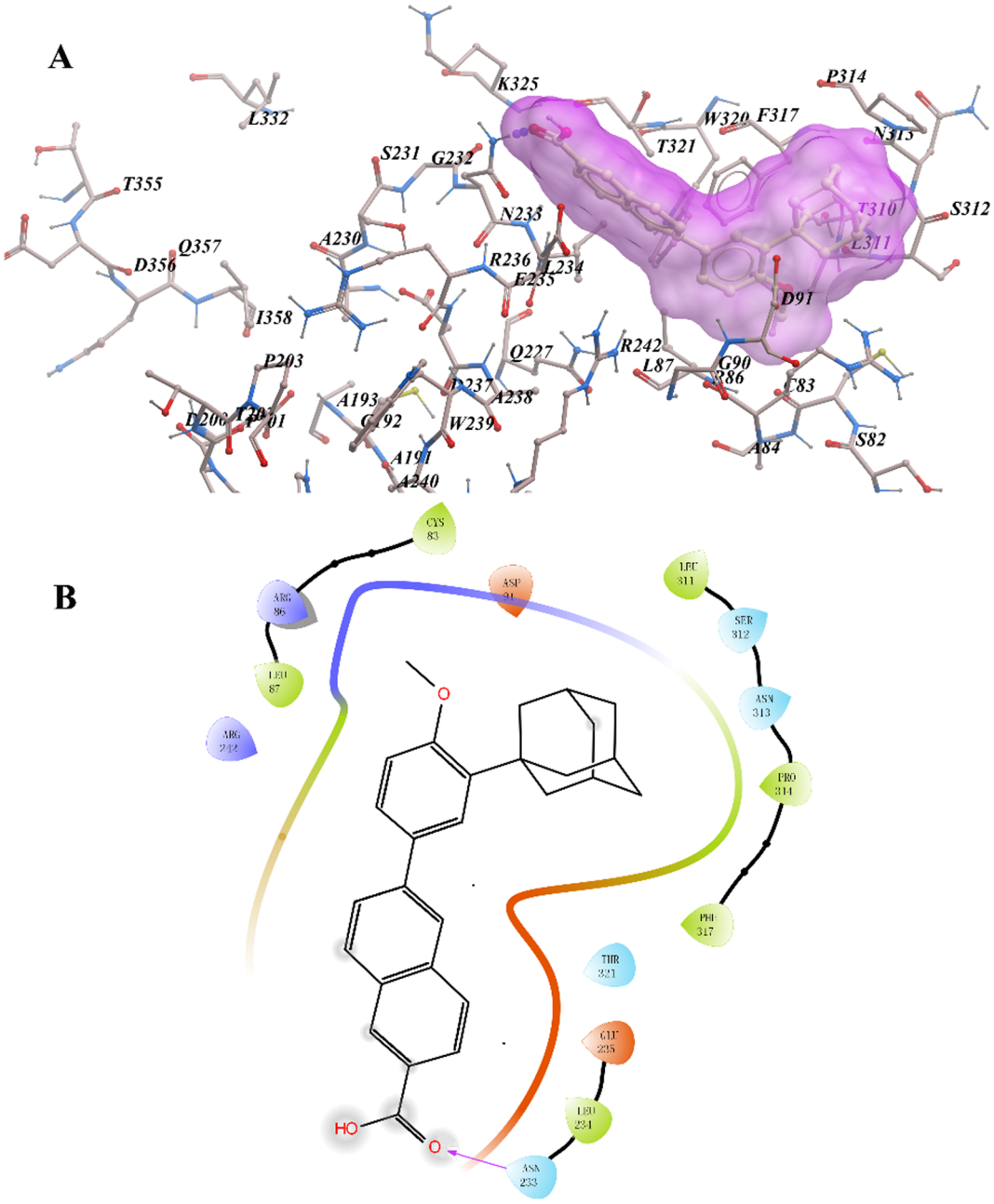

Fig. 4. The low-energy binding conformations of ADA bound to GOT1 generated by molecular docking. (A) Detailed view of ADA binding in the active site of GOT1. (B) Ligand interaction diagram of ADA with GOT1.

cancer (Hep3B), cervical cancer (Hela), ovarian cancer (HOV-7, ES-2), normal cells (CHO, L929) and so on. High expression levels of GOT1 were observed in some of these cell lines (Fig. 5A). The growth inhibitory effects of ADA on each cell line were measured by MTT, and obtained IC_{50} values were presented in Table 2. In combination with the expression level of GOT1 protein in these cancer cells, we can know that ADA is more sensitive to cancer cells with higher GOT1 protein expression. As displayed in Fig. 5B, C, D, E, ES-2 cells with higher expression of GOT1 showed more obvious sensitivity to ADA (IC_{50} = 10.36 ± 1.16 μM) than Chinese hamster ovary (CHO) cells. Furthermore, three normal cell lines, including LO2, Vero, L929, were also used to detect the cytotoxicity of ADA for assessing the safety of ADA. As shown in Fig. 5E, the IC_{50} values of ADA on normal tissue cells were much higher than that of ES-2 cells by 5 folds. The selectivity and security of ADA make it a potential drug for treating ovarian cancer.

To investigate the growth-promoting role of GOT1 in cancer cells, the expression of GOT1 was knocked down in ES-2 cancer cells. ES-2 cells transfected with siRNA 2-3 down-regulated GOT1 expression compared to siRNA transfected control (siCtrl) (Fig. 5F). Effects of ADA on the growth of siCtrl and shGOT1 transfected ES-2 were assessed by MTT. Results indicated that cells transfected with shGOT1 were resistant to the inhibitory effect of ADA on the growth compared with cells transfected with siCtrl (Fig. 5G). These findings suggested that anticancer activities induced by ADA were dependent on the GOT1 expression.

3.6. ADA induced ES-2 cells apoptosis and inhibited proliferation in vitro

To elucidate the mechanisms of ADA-induced growth inhibition of ES-2 cells, the cells were stained with Hoechst 33258 to determine the incidence of apoptosis morphologically. The ADA-treated groups showed a significant increase in apoptosis compared with the control

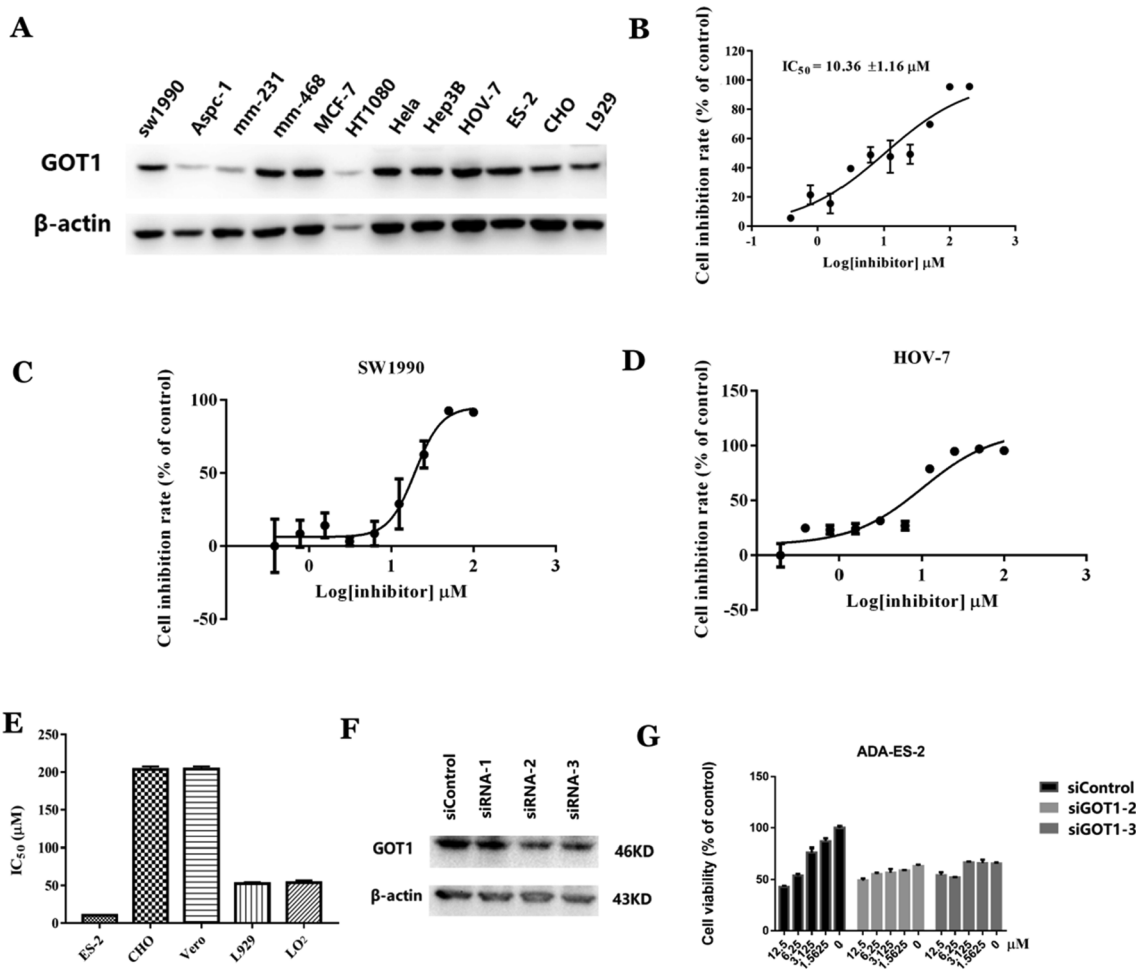

Fig. 5. *In vitro* antiproliferative activity of ADA. (A) Expression of GOT1 in pancreatic cancer, breast cancer, liver cancer, cervical cancer, ovarian cancer and normal cells. β-actin was examined to serve as a loading control. (B-C) The affections of ADA on ES-2, SW1990 and HOV-7 cells detected by MTT assays. (D) Graph indicates IC_{50} values of ADA in ES-2, CHO, Vero, L929, LO2 cell lines. (E) Knock down of GOT1 using siRNA in ES-2 cells followed by western blotting revealed the protein expression levels of GOT1, compared with the siRNA-transfected control. (F) ES-2 cells were transfected with siRNA2-3 or siCtrl followed by treatment with ADA. Cell viability was analyzed.

Table 2
The inhibition of ADA on all kinds of cells.

Cell	ADA (μM)
SW1990	19.52 ± 1.29
AsPC-1	≈50
MM-231	> 50
MM-468	31.47 ± 1.31
MCF-7	12.00 ± 1.23
HT1080	21.70 ± 1.08
Hela	19.08 ± 1.24
Hep3B	> 50
HOV-7	10.81 ± 0.99
ES-2	10.36 ± 1.16
SW480	> 50
SW620	> 50
HCT116	≈100
PANC-1	≈50
A549	> 50
L929	> 50
LO2	> 50
Vero	> 200
HPDE6C7	> 50

group (Fig. 6C). Especially, chromatin condensation in ES-2 cells after treated with ADA indicated that ADA increased the extent of apoptosis. Additionally, Western blot analysis showed the expression of anti-apoptotic protein Bcl-2 and PARP were down regulated with the treatment of ADA in a dose-dependent manner in ES-2 cells (Fig. 6A), suggesting that ADA induced cell death through Bcl-2 mediated apoptosis. The quantization ratio of Bcl-2 and PARP to β-actin was shown respectively in Fig. 6B.

In the subsequent experiments, the proliferation of ES-2 cells was detected by cloning formation assay. ADA significantly decreased the proliferation of ES-2 cells at 10 μM compared with the control group ($p < 0.001$, Fig. 7A). EdU and DAPI double staining experiments showed that ADA significantly inhibited the proliferation of ES-2 cells at the concentration of 10 μM and 20 μM. As shown in Fig. 7C, the number of EdU^+ positive cells in ES-2 cells decreased after treated with ADA.

3.7. ADA inhibited ES-2 cells migration in a dose-dependent manner

One of the reasons for the difficulty in treating ovarian cancer is its high metastasis, so we conducted the transwell assay to verify if ADA could inhibit the migration of ES-2 cells. As revealed in Fig. 8A, the metastasis of ES-2 cells from upper chamber to lower chamber was suppressed by ADA in a dose-dependent manner. Additionally, the scratch wound assay displayed that ADA markedly reduced the wound healing abilities of ES-2 cells (Fig. 8B), which was in accordance with the above results in transwell assay.

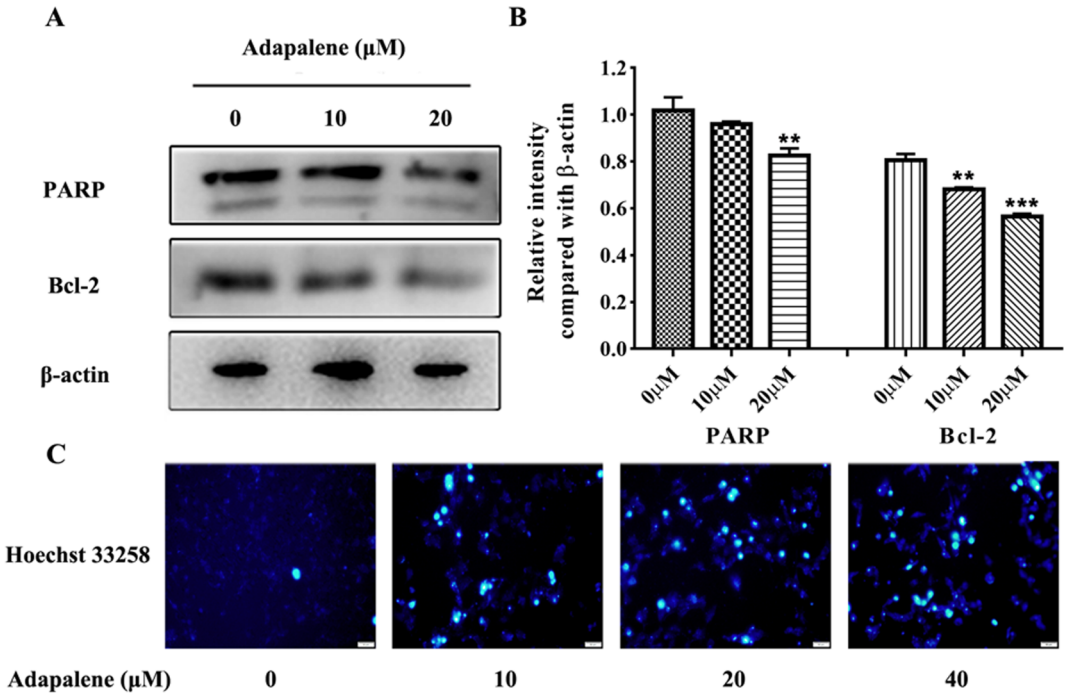

Fig. 6. Apoptosis induced by treatment of ADA (10–40 μM). (A) and (B) The level of apoptosis-associated proteins treated with ADA detected by Western blot and quantitative analysis. The asterisk ** indicated $p < 0.01$, and the asterisk *** indicated $p < 0.001$. (C) The Hoechst 33258 strained of ES-2 after treated with ADA or 1% DMSO.

4. Discussion and conclusion

Deregulation of metabolism is a hallmark of cancers [27]. Adaption to the microenvironment and the nutrient levels constantly changing in solid tumors are important for the survival of tumor cells [28]. Research on cell metabolism promoting tumors growth have has shown become a selective anticancer strategy that targeting on metabolic dependencies of cancer cells [29]. GOT1 plays a crucial role in the metabolic

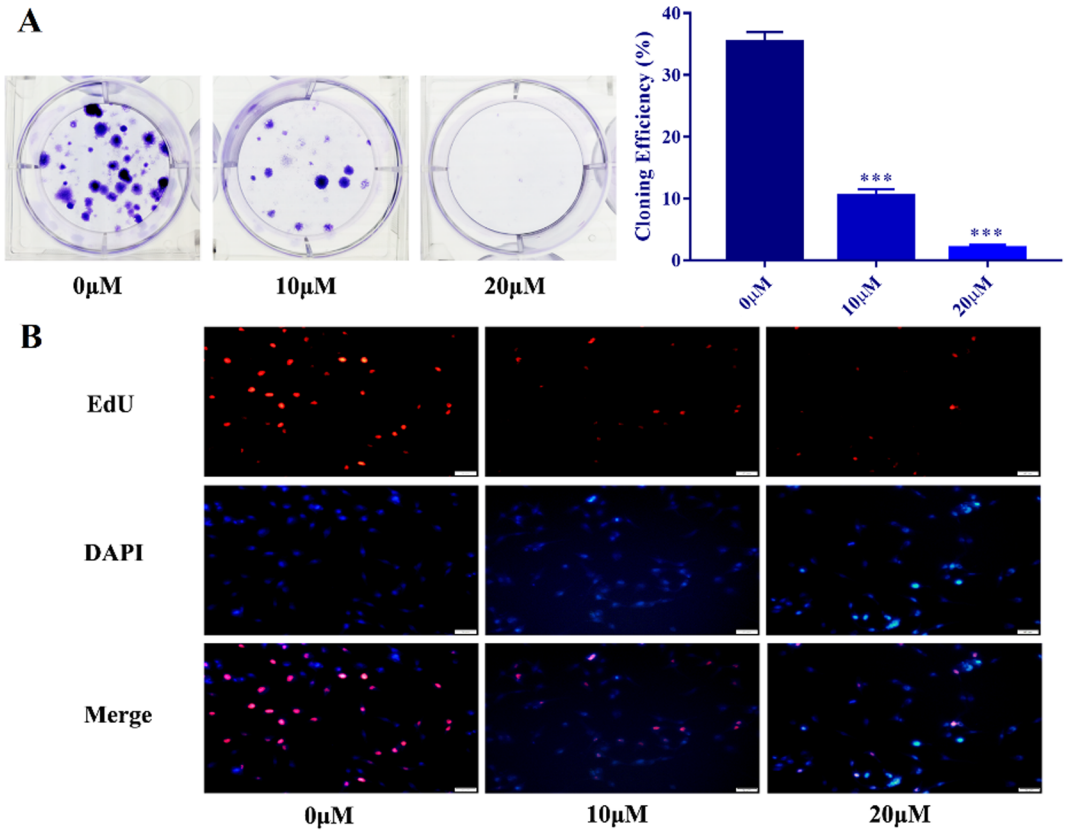

Fig. 7. ADA inhibited ES-2 cell proliferation. (A) The cloning formation assay and quantitative analysis of ES-2 cells after treated with ADA (10 μM and 20 μM, respectively). (B) The percentage of cell proliferation was detected by EdU assay. The asterisk *** indicated $p < 0.001$.

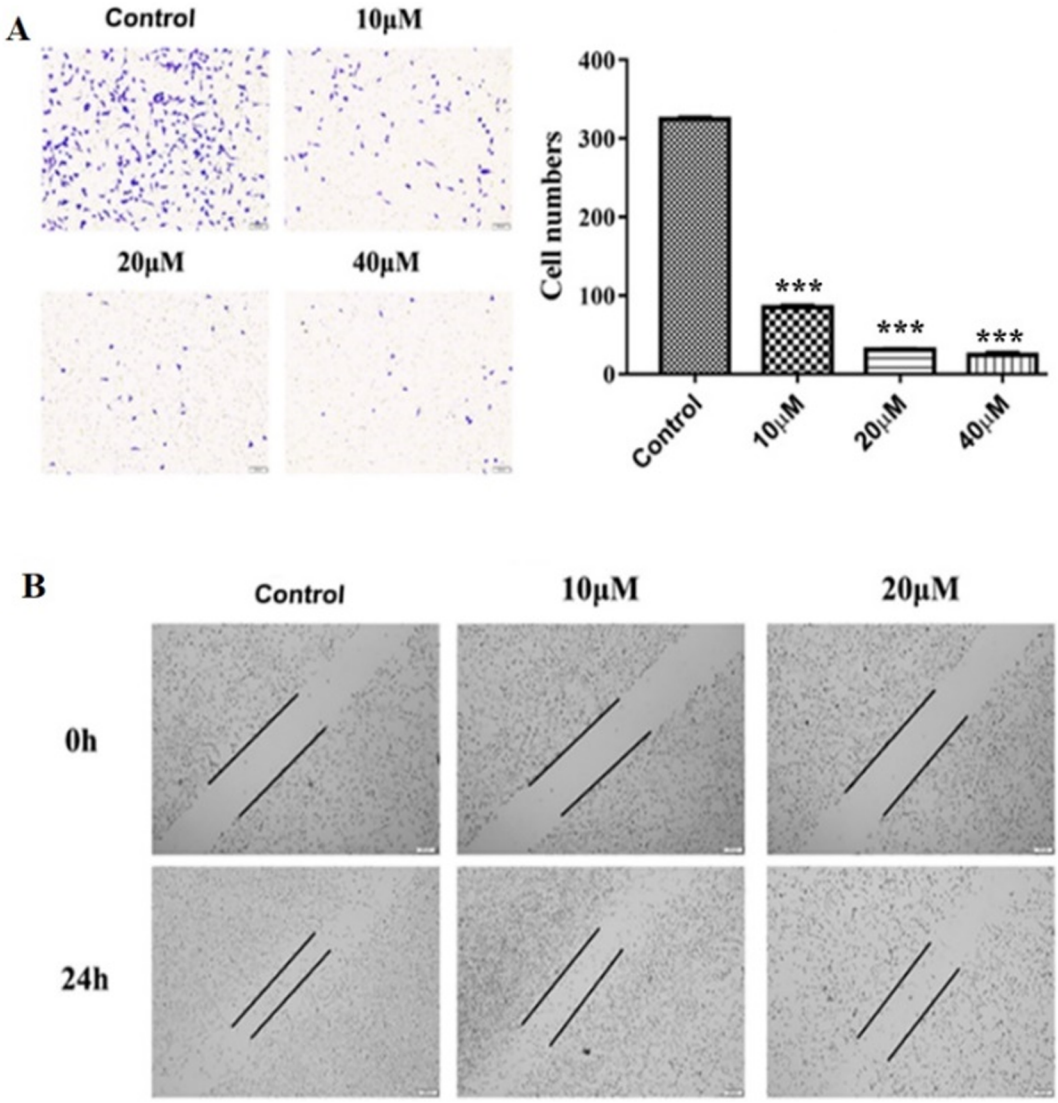

Fig. 8. ADA inhibited the ES-2 cells migration *in vitro*. (A) Transwell assay and quantitatively analysis. (B) The scratch wound healing images were taken at 0 h and 24 h post-scratch using a phase contrast microscope with a Nikon camera. *** $p < 0.001$.

reprogramming, and the inhibitors of GOT1 could suppress tumor cell proliferation [30]. However, few GOT1 inhibitors have been found, and the related researches remain in the initial stage [31].

Drug repurposing is re-investigating the new therapeutic indications of the existing approved drugs. This strategy is propitious to identify new therapies for diseases at lower cost and in a shorter time, exceptionally it may have diversified preclinical safety studies. Thus, it holds the great potential in overcoming hurdles during drug research and development [32].

In this work, we first reported that ADA, as a dermatological drug approved by FDA, inhibited activity of GOT1 in a non-competitive manner. Molecular docking, MST assay, and DARTS further revealed that ADA behaved an affinity to GOT1. Therefore, ADA was determined as an effective GOT1 inhibitor. More excitingly, we can know that ADA is more sensitive to cancer cells with higher GOT1 protein expression. And the inhibition of GOT1 by ADA is dependent on the abundance of GOT1. Correspondingly, ADA also inhibited the migration and induced apoptosis of ES-2 cells *in vitro*. All the results provided a novel therapeutic strategy for ovarian cancer, also represented the first drug repurposing inhibitor of GOT1.

Compared with other existing inhibitors of GOT1, such as iGOT1-01, ADA could be used directly as a drug candidate for indication treatment or as a lead compound to further synthesize more effective inhibitors through structural modifications. The light stability of ADA is five times higher than that of natural vitamin A. Its toxicity profile is also more favorable than other retinoids, the oral LD_{50} of rats and mice is 5 g/kg. Even a large amount of oral ADA does not cause any neurological, hematological, cardiovascular or respiratory side effects [15]. Although the inhibition of a series of iGOT1-01 analogs on GOT1 was assessed, their anticancer activity *in vitro* and *in vivo* hadn't been evaluated yet [33]. Li et al. demonstrated that S phase arrest mediated by DNA damage was the main mechanism for the proliferation inhibition of melanoma cells by ADA, but it is only a hypothesis that the real target of ADA anticancer remains to be explored. We proved that GOT1 was the target of action of ADA through experiments, and according to other articles, this inhibitory effects were independent of the activation of RAR and RXR [34].

In conclusion, we discovered a novel action mode of ADA that efficiently inhibited proliferation and enhanced apoptosis in ES-2 cells *in vitro*. Consequently, ADA may contribute to the adjunctive therapeutics

for advanced stages of ovarian cancer by targeting GOT1. The discovery of ADA as a GOT1 inhibitor might greatly reduce the cost of R&D of new antitumor drugs, and it provides more insights in the further ADA-based designs to produce more potent and selective novel drug for ovarian cancer therapy.

Declaration of Competing Interest

The authors claim that the researchers in this study have no conflict of interest.

Acknowledgements

We acknowledge support from National Natural Science Foundation of China (NSFC) (grant number 81773594, 31270399, U1703111, U1803122, 81773637 and 81903863), the Fundamental Research Fund for the Central Universities (grant number 2017KFYXJJ151), Liaoning Province Natural Science Foundation (grant number 201602689), China Postdoctoral Science Foundation (grant number 2019M652661). We acknowledge support from Schrödinger Release 2018-4: Maestro, Schrödinger, LLC, New York, NY, 2018.

References

[1] R.L. Siegel, K.D. Miller, A. Jemal, Cancer statistics, 2016, CA Cancer J. Clin. 66 (1) (2016) 7–30.
[2] X.S. Zhou, et al., Inhibition of glutamate oxaloacetate transaminase 1 in cancer cell lines results in altered metabolism with increased dependency of glucose, BMC Cancer (2018) 18.
[3] Y. Collins, et al., Gynecologic cancer disparities: a report from the Health Disparities Taskforce of the Society of Gynecologic Oncology, Gynecol. Oncol. 133 (2) (2014) 353–361.
[4] M.G.V. Heiden, L.C. Cantley, C.B. Thompson, Understanding the Warburg effect: the metabolic requirements of cell proliferation, Science 324 (5930) (2009) 1029–1033.
[5] M. Israel, On the origin of cancers by means of metabolic selection. Tumor cell targets, Biomed. Res.-India 23 (2012) 5–8.
[6] D. Hanahan, R.A. Weinberg, Hallmarks of cancer: the next generation, Cell 144 (5) (2011) 646–674.
[7] S. Tardito, et al., Glutamine synthetase activity fuels nucleotide biosynthesis and supports growth of glutamine-restricted glioblastoma, Nat. Cell Biol. 17 (12) (2015) 1556–1568.
[8] J. Abrego, et al., GOT1-mediated anaplerotic glutamine metabolism regulates chronic acidosis stress in pancreatic cancer cells, Cancer Lett. 400 (2017) 37–46.
[9] L.E. Millikan, Adapalene: an update on newer comparative studies between the various retinoids, Int. J. Dermatol. 39 (10) (2000) 784–788.
[10] S.V. Bershad, The modern age of acne therapy: a review of current treatment options, Mt. Sinai J. Med. 68 (4–5) (2001) 279–286.
[11] R.N. Brogden, K.L. Goa, Adapalene - a review of its pharmacological properties and clinical potential in the management of mild to moderate acne, Drugs 53 (3) (1997) 511–519.
[12] S. Michel, A. Jomard, M. Demarchez, Pharmacology of adapalene, Br. J. Dermatol. 139 (1998) 3–7.
[13] B. Shroot, S. Michel, Pharmacology and chemistry of adapalene, J. Am. Acad. Dermatol. 36 (6) (1997) S96–S103.
[14] M. Ocker, et al., Potentiated anticancer effects on hepatoma cells by the retinoid adapalene, Cancer Lett. 208 (1) (2004) 51–58.
[15] M. Ocker, et al., The synthetic retinoid adapalene inhibits proliferation and induces apoptosis in colorectal cancer cells in vitro, Int. J. Cancer 107 (3) (2003) 453–459.
[16] Y.T. Ye, et al., Apoptosis induced by the methanol extract of Salvia miltiorrhiza Bunge in non-small cell lung cancer through PTEN-mediated inhibition of PI3K/Akt pathway, J. Ethnopharmacol. 200 (2017) 107–116.
[17] Z. Li, et al., The dietary compound luteolin inhibits pancreatic cancer growth by targeting BCL-2, Food Funct. 9 (5) (2018) 3018–3027.
[18] X. Jiang, H. Chang, Y. Zhou, Expression, purification and preliminary crystallographic studies of human glutamate oxaloacetate transaminase 1 (GOT1), Protein Expr. Purif. 113 (2015) 102–106.
[19] Q. Wang, et al., Rational design of selective allosteric inhibitors of PHGDH and serine synthesis with anti-tumor activity, Cell Chem. Biol. 24 (1) (2017) 55–65.
[20] M.Y. Pai, et al., Drug affinity responsive target stability (DARTS) for small-molecule target identification, Meth. Mol. Biol. 1263 (2015) 287–298.
[21] Q. Min, et al., Identification of mangiferin as a potential Glucokinase activator by structure-based virtual ligand screening, Sci. Rep. 7 (2017) 44681.
[22] Q.P. Peng, et al., Stable RNA interference of hexokinase II gene inhibits human colon cancer LoVo cell growth in vitro and in vivo, Cancer Biol. Ther. 7 (7) (2008) 1128–1135.
[23] B. Ruster, et al., Induction and detection of human mesenchymal stem cell migration in the 48-well reusable transwell assay, Stem Cells Dev. 14 (2) (2005) 231–235.
[24] C.C. Liang, A.Y. Park, J.L. Guan, In vitro scratch assay: a convenient and inexpensive method for analysis of cell migration in vitro, Nat. Protoc. 2 (2) (2007) 329–333.
[25] D. Mahendiran, et al., In vitro and in vivo anti-proliferative evaluation of bis(4'-(4-tolyl)-2,2':6',2aEuro(3)-terpyridine)copper(II) complex against Ehrlich ascites carcinoma tumors, J. Biol. Inorg. Chem. 22 (7) (2017) 1109–1122.
[26] F. Hirasawa, et al., Styrene monomer primarily induces CYP2B1 mRNA in rat liver, Xenobiotica 35 (12) (2005) 1089–1099.
[27] C.V. Dang, Links between metabolism and cancer, Genes Dev. 26 (9) (2012) 877–890.
[28] N.N. Pavlova, C.B. Thompson, The emerging hallmarks of cancer metabolism, Cell Metab. 23 (1) (2016) 27–47.
[29] M.G. Vander Heiden, Targeting cancer metabolism: a therapeutic window opens, Nat. Rev. Drug Discov. 10 (9) (2011) 671–684.
[30] G. Chakrabarti, et al., Targeting glutamine metabolism sensitizes pancreatic cancer to PARP-driven metabolic catastrophe induced by ss-lapachone, Cancer Metab. 3 (2015) 12.
[31] J. Anglin, et al., Discovery and optimization of aspartate aminotransferase 1 inhibitors to target redox balance in pancreatic ductal adenocarcinoma, Bioorg. Med. Chem. Lett. 28 (16) (2018) 2675–2678.
[32] Y. Cha, et al., Drug repurposing from the perspective of pharmaceutical companies, Br. J. Pharmacol. 175 (2) (2018) 168–180.
[33] M.C. Holt, et al., Biochemical characterization and structure-based mutational analysis provide insight into the binding and mechanism of action of novel aspartate aminotransferase inhibitors, Biochemistry 57 (47) (2018) 6604–6614.
[34] H. Li, C. Wang, L. Li, et al., Adapalene suppressed the proliferation of melanoma cells by S-phase arrest and subsequent apoptosis via induction of DNA damage, Eur. J. Pharmacol. 851 (2019) 174–185.